


Subshell Ordering and Periodic Structure from Time-Scalar Field Theory

Jordan G. Farrell 
Independent Researcher
Colchester, Connecticut, USA
jgfquantum@gmail.com

April 24, 2026

Abstract

We analyze the emergence of atomic spectral structure within the framework of Time-Scalar Field Theory (TSFT) by considering fluctuations about localized static scalar-time configurations. The asymptotic behavior of the background field induces an effective radial operator whose leading contribution yields an inverse-radial interaction and a degenerate spectrum characterized by the principal quantum number n .

Extending the asymptotic expansion to next order produces a subleading $1/r^2$ correction determined by higher derivatives of the scalar-time potential. Using an exact evaluation of the expectation value $\langle r^{-2} \rangle$ via the Hellmann–Feynman theorem, we obtain a closed-form expression for the subshell-dependent energy shifts and derive the corrected spectrum

$$\varepsilon_{n\ell} = -\frac{\kappa^2}{4n^2} + \frac{\beta\kappa^2}{4n^3 \left(\ell + \frac{1}{2}\right)}.$$

This structure lifts the degeneracy within each principal shell, producing a systematic ordering of subshells by angular momentum. The ordering of subshells belonging to different principal shells is shown to depend on the balance between the leading and subleading contributions. By analyzing the resulting energy inequalities, we derive explicit conditions on the subleading coefficient β under which cross-shell inversions consistent with the observed periodic hierarchy occur.

The coefficient β is expressed in terms of the fourth derivative of the scalar-time potential, allowing the ordering conditions to be recast as constraints on the local curvature structure of the underlying field. In this formulation, principal shell structure is governed by the cubic derivative of the potential, while subshell ordering and periodic organization arise from its quartic derivative.

These results establish that key features of atomic structure—shell degeneracy, subshell splitting, and conditional periodic ordering—emerge from the scalar-time framework without the introduction of empirical filling rules. The analysis reduces the problem of atomic periodicity to a concrete constraint on the derivative structure of the scalar-time potential, providing a direct link between field dynamics and observed atomic organization.

1 Introduction

The structure of the periodic table is one of the central organizing principles of atomic physics. While the gross features of atomic spectra are well understood in terms of the Coulomb interaction and quantum mechanics, the detailed ordering of subshell energies within and across principal

shells is typically described using empirical rules, such as the Madelung (or $(n + \ell)$) rule, together with phenomenological corrections attributed to electron-electron interactions and screening effects. These rules successfully reproduce observed atomic structure, but they are not derived from first principles in a fully unified manner.

In previous work, Time-Scalar Field Theory (TSFT) was shown to produce the hydrogenic spectral structure without assuming a Coulomb potential or postulating quantum mechanical operators. Starting from the scalar-time field equation, localized static configurations were constructed, and the induced fluctuation operator governing perturbations about these backgrounds was derived. The asymptotic expansion of this operator yielded an inverse-radial interaction, leading to a Sturm–Liouville problem whose normalizable solutions produce a discrete spectrum of the form

$$\varepsilon_n = -\frac{\kappa^2}{4n^2},$$

together with shell degeneracies consistent with the $2n^2$ structure of atomic states.

That result establishes the principal shell structure as a consequence of scalar-time field dynamics. However, the observed organization of atomic structure depends not only on the principal quantum number n , but also on the ordering of subshells characterized by the angular momentum quantum number ℓ . Within a given principal shell, the degeneracy of states with different ℓ must be lifted, and across shells, competing energy scales determine the sequence in which subshells are filled. In standard treatments, this structure is attributed to corrections beyond the idealized Coulomb problem, including relativistic effects, spin-orbit coupling, and many-body interactions.

The purpose of the present work is to derive the origin of subshell ordering directly from TSFT, without introducing empirical filling rules or independently postulated interaction terms. We focus on the subleading structure of the scalar-time background and its effect on the radial fluctuation operator. Expanding the induced operator beyond leading order reveals corrections of order $1/r^2$, which modify the effective potential governing bound states. These corrections provide a natural mechanism for lifting the degeneracy within each principal shell.

Rather than redefining the angular momentum structure, we treat the subleading contributions within a controlled perturbative framework. The unperturbed eigenfunctions obtained from the inverse-radial problem form a complete basis, allowing the computation of subshell-dependent energy shifts through expectation values of the perturbing operator. This approach preserves the exact solvability of the leading-order problem while introducing well-defined corrections that encode the detailed structure of atomic spectra.

We show that the resulting energy shifts depend explicitly on both the principal quantum number n and the angular momentum quantum number ℓ , and that their scaling induces a systematic ordering of subshell energies. Moreover, the same structure produces competition between subshells belonging to different principal shells, yielding ordering patterns consistent with those observed in the periodic table. In this way, the empirical hierarchy of atomic structure is recovered as a consequence of the spatial structure of the scalar-time field and the properties of its induced fluctuation operator.

The analysis presented here is restricted to the single-particle sector in the presence of a localized source, and therefore does not include explicit many-body effects. Nonetheless, it demonstrates that the primary organization of subshell energies arises at the level of the underlying field structure. Additional effects, such as electron-electron interactions and relativistic corrections, may be incorporated as higher-order refinements, but are not required to explain the leading ordering pattern.

Accordingly, this work extends the TSFT program from the derivation of principal shell structure to the determination of subshell ordering, providing a unified and non-circular framework for

the emergence of atomic periodicity from first principles.

2 Radial Operator and Leading-Order Structure

We briefly summarize the radial structure governing bound states in the scalar-time framework, as established in prior work, in order to provide a self-contained basis for the analysis that follows.

Fluctuations about a static, spherically symmetric scalar-time background $\Theta_0(r)$ are governed by a second-order differential operator of the form

$$\left[-\frac{d^2}{dr^2} + \frac{\ell(\ell+1)}{r^2} + V''(\Theta_0(r)) \right] u(r) = \omega^2 u(r),$$

where $u(r)$ is the reduced radial function and ℓ is the angular momentum quantum number arising from separation of variables in spherical coordinates.

For localized sources, the background field admits the asymptotic form

$$\Theta_0(r) = \Theta_\infty + \frac{A}{r},$$

which leads, upon expansion of $V''(\Theta_0(r))$ about Θ_∞ , to the effective radial operator

$$-\frac{d^2}{dr^2} + \left[\frac{\ell(\ell+1)}{r^2} - \frac{\kappa}{r} \right] u(r) = \varepsilon u(r),$$

after absorbing the constant term $V''(\Theta_\infty)$ into the spectral parameter and defining $\kappa = -AV'''(\Theta_\infty) > 0$ under the binding condition.

This operator defines the leading-order bound-state problem. Its solutions are obtained by standard Sturm–Liouville methods, and normalizability imposes a quantization condition that yields the discrete spectrum

$$\varepsilon_n = -\frac{\kappa^2}{4n^2},$$

with principal quantum number $n = 1, 2, 3, \dots$

At this level, the spectrum depends only on n , and states with different angular momentum ℓ within the same principal shell are degenerate. The degeneracy arises from the fact that the leading-order operator depends on ℓ only through the centrifugal term, while the inverse-radial interaction introduces no additional ℓ -dependence in the energy eigenvalues.

Thus, the leading-order structure reproduces the principal shell organization of atomic spectra but does not determine the ordering of subshells. The lifting of this degeneracy requires consideration of subleading contributions to the effective radial operator, which are derived in the following section.

3 Subleading Scalar-Time Corrections

We derive the first subleading contribution to the effective radial operator by expanding $V''(\Theta_0(r))$ about the asymptotic value Θ_∞ to one order beyond the leading term.

For localized sources, the background field has the asymptotic form

$$\Theta_0(r) = \Theta_\infty + \frac{A}{r}.$$

Substituting into $V''(\Theta_0)$ and performing a Taylor expansion about Θ_∞ yields

$$V''(\Theta_0(r)) = V''(\Theta_\infty) + V'''(\Theta_\infty) \frac{A}{r} + \frac{1}{2} V^{(4)}(\Theta_\infty) \frac{A^2}{r^2} + O\left(\frac{1}{r^3}\right).$$

As in the leading-order analysis, the constant term $V''(\Theta_\infty)$ is absorbed into the spectral parameter. The first-order term produces the inverse-radial interaction

$$-\frac{\kappa}{r}, \quad \kappa = -A V'''(\Theta_\infty) > 0,$$

under the binding condition.

The next term in the expansion yields a correction of order $1/r^2$, which we write as

$$\frac{\beta}{r^2}, \quad \beta = \frac{1}{2} A^2 V^{(4)}(\Theta_\infty).$$

Thus, the effective radial operator including subleading corrections becomes

$$-\frac{d^2}{dr^2} + \left[\frac{\ell(\ell+1)}{r^2} - \frac{\kappa}{r} + \frac{\beta}{r^2} \right] u(r) = \varepsilon u(r),$$

up to terms of order $O(r^{-3})$.

The $1/r^2$ contribution arises from the intrinsic curvature of the scalar-time potential at the asymptotic background and is therefore determined entirely by the underlying TSFT Lagrangian. No additional interaction terms have been introduced.

Importantly, the correction appears at the same order as the centrifugal term. However, we do not absorb β into a redefinition of the angular momentum quantum number. Such a redefinition would, in general, destroy the integer structure required for polynomial termination of the radial solutions. Instead, we treat the β/r^2 term as a perturbation to the leading-order operator.

This preserves the exact solvability of the inverse-radial problem while allowing controlled computation of subshell-dependent energy shifts, which are derived in the following section.

4 Perturbative Spectrum and Subshell Energy Shifts

The subleading correction derived in the previous section introduces an additional term of the form β/r^2 into the effective radial operator. To determine its effect on the energy spectrum, we treat this contribution within first-order perturbation theory, using the eigenfunctions of the leading-order inverse-radial problem as the unperturbed basis.

Let $\psi_{n\ell}(r)$ denote the normalized eigenfunctions of the operator

$$-\frac{d^2}{dr^2} + \left[\frac{\ell(\ell+1)}{r^2} - \frac{\kappa}{r} \right],$$

with corresponding eigenvalues

$$\varepsilon_n = -\frac{\kappa^2}{4n^2}.$$

The first-order correction to the energy is

$$\Delta_{n\ell} = \left\langle \psi_{n\ell} \left| \frac{\beta}{r^2} \right| \psi_{n\ell} \right\rangle = \beta \left\langle \frac{1}{r^2} \right\rangle_{n\ell}.$$

Thus, the problem reduces to evaluating the expectation value $\langle r^{-2} \rangle_{n\ell}$ with respect to the unperturbed eigenfunctions.

For bound states of the inverse-radial operator, the exact expectation value is derived in Appendix C using the Hellmann–Feynman theorem:

$$\left\langle \frac{1}{r^2} \right\rangle_{n\ell} = \frac{\kappa^2}{4n^3 \left(\ell + \frac{1}{2}\right)}.$$

Substituting this result gives the exact first-order subshell shift

$$\Delta_{n\ell} = \frac{\beta\kappa^2}{4n^3 \left(\ell + \frac{1}{2}\right)}.$$

Accordingly, the corrected energy spectrum is

$$\varepsilon_{n\ell} = -\frac{\kappa^2}{4n^2} + \frac{\beta\kappa^2}{4n^3 \left(\ell + \frac{1}{2}\right)}.$$

Equivalently,

$$\varepsilon_{n\ell} = \kappa^2 \left[-\frac{1}{4n^2} + \frac{\beta}{4n^3 \left(\ell + \frac{1}{2}\right)} \right].$$

This expression shows explicitly that the leading degeneracy within each principal shell is lifted by the subleading scalar-time correction. The magnitude and sign of the splitting are governed by the coefficient β , while the dependence on n and ℓ is fixed by the spectral structure of the unperturbed inverse-radial operator.

5 Subshell Ordering

Remark on perturbative validity. The perturbative treatment assumes that the subleading correction β/r^2 produces small shifts relative to the leading inverse-radial problem. However, the ordering conditions derived in Appendix D require values of β whose magnitude is not parametrically small for low- ℓ states, particularly $\ell = 0$.

Accordingly, the present analysis should be interpreted as identifying the mechanism and parameter regime suggested by first-order perturbation theory, rather than as a strictly controlled expansion in that regime. A fully non-perturbative treatment, based on the exact spectrum of the modified radial operator, would provide a more rigorous determination of the ordering structure and is left for future work.

The perturbative result obtained in the previous section shows that the degeneracy of the leading-order spectrum is lifted by a subshell-dependent correction of the form

$$\Delta_{n\ell} = \frac{\beta\kappa^2}{4n^3 \left(\ell + \frac{1}{2}\right)}.$$

We now examine the consequences of this correction for the ordering of subshell energies.

5.1 Intra-Shell Ordering

For a fixed principal quantum number n , the leading contribution

$$-\frac{\kappa^2}{4n^2}$$

is constant, so the ordering within a shell is determined entirely by the subleading correction.

Thus, for fixed n ,

$$\varepsilon_{nl} = -\frac{\kappa^2}{4n^2} + \frac{\beta\kappa^2}{4n^3\left(\ell + \frac{1}{2}\right)}.$$

The dependence on ℓ is therefore governed by

$$\frac{1}{\ell + \frac{1}{2}},$$

which is strictly decreasing in ℓ .

Accordingly, for $\beta < 0$, one obtains

$$\varepsilon_{n,0} < \varepsilon_{n,1} < \varepsilon_{n,2} < \dots,$$

corresponding to the ordering

$$s < p < d < f$$

within each principal shell.

Thus, the scalar-time correction produces a systematic lifting of degeneracy that orders subshells by angular momentum.

5.2 Cross-Shell Ordering

The ordering of subshells belonging to different principal shells cannot be determined from the perturbative correction alone. Instead, it requires comparison of the full energy expression

$$\varepsilon_{nl} = -\frac{\kappa^2}{4n^2} + \frac{\beta\kappa^2}{4n^3\left(\ell + \frac{1}{2}\right)}.$$

In this case, the leading term favors lower values of n , while the subleading term introduces an ℓ -dependent correction that may shift the relative ordering of states.

Accordingly, the ordering of two subshells (n, ℓ) and (n', ℓ') is determined by the inequality

$$-\frac{1}{4n^2} + \frac{\beta}{4n^3\left(\ell + \frac{1}{2}\right)} < -\frac{1}{4n'^2} + \frac{\beta}{4n'^3\left(\ell' + \frac{1}{2}\right)}.$$

The analysis of this condition is carried out in Appendix D, where explicit bounds on the coefficient β are derived for representative subshell pairs.

5.3 Role of the Subleading Coefficient

The results of Appendix D show that cross-shell inversions occur when the magnitude of the subleading correction is sufficiently large to overcome the difference in principal energy levels.

In particular, the observed ordering of subshells in atomic systems corresponds to a regime in which β is negative and satisfies a set of explicit inequality constraints.

Thus, while intra-shell ordering follows directly from the angular dependence of the perturbative correction, cross-shell ordering is governed by a balance between the principal scaling and the subleading scalar-time contribution.

5.4 Summary

The scalar-time framework therefore produces two distinct structural effects. First, degeneracy is lifted within each shell, yielding the ordering $s < p < d < f$. Second, cross-shell ordering arises conditionally, governed by the magnitude of the subleading coefficient β .

The first effect is universal within the present framework, while the second depends on the detailed structure of the scalar-time potential and is analyzed quantitatively in Appendix D.

6 Emergence of Periodic Structure

The subshell ordering derived in the previous section provides a structural basis for the organization of atomic states. We now connect this ordering to the emergence of periodic structure within the scalar-time framework.

6.1 Shell Capacities

At leading order, the degeneracy of the principal shell n is

$$g_n = 2n^2,$$

where the factor of two accounts for the intrinsic two-component structure of fermionic excitations. This determines the total number of states available within each shell.

Within a given shell, the number of states associated with a subshell of angular momentum ℓ is

$$g_{n\ell} = 2(2\ell + 1),$$

arising from the $(2\ell + 1)$ angular modes together with the two-component internal structure.

These capacities follow directly from the symmetry structure of the scalar-time fluctuation operator and are independent of subleading corrections.

6.2 Energy Ordering and Filling Sequence

The sequence in which subshells are occupied is determined by their relative energies. As shown in Section 5, the corrected energy spectrum is

$$\varepsilon_{n\ell} = -\frac{\kappa^2}{4n^2} + \frac{\beta\kappa^2}{4n^3(\ell + \frac{1}{2})}.$$

The ordering of subshells is therefore governed by the full energy expression, rather than by the scaling of the perturbative correction alone. While the quantity $n^3(\ell + \frac{1}{2})$ provides a useful indicator of the relative size of the subleading contribution, the actual ordering follows from the balance between the principal term and the subshell-dependent correction.

In particular, cross-shell ordering is determined by the inequality derived in Section 5 and analyzed quantitatively in Appendix D, which yields explicit conditions on the coefficient β under which subshell inversions occur.

6.3 Periodic Structure

The periodic nature of atomic structure arises from the repeated filling of states within shells of capacity $2n^2$. As subshells are filled according to their energy ordering, the resulting configuration exhibits recurring patterns in the occupation of angular momentum states.

These patterns manifest as distinct blocks corresponding to subshell types, whose lengths are determined by their degeneracies:

$$s : 2, \quad p : 6, \quad d : 10, \quad f : 14.$$

Thus, the block structure of the periodic table follows directly from the angular momentum decomposition of the scalar-time fluctuation operator, while the sequence of these blocks is determined by the energy ordering governed by the scalar-time dynamics.

6.4 Scope of the Derivation

The present analysis establishes that the primary organization of atomic structure—shell capacities, subshell decomposition, and conditional ordering—arises from the scalar-time field and its induced operator structure.

The treatment is restricted to the single-particle sector in the presence of a localized source. Additional effects, including electron-electron interactions, spin-orbit coupling, and relativistic corrections, may modify detailed energy levels. However, the leading hierarchical structure is determined at the level of the underlying scalar-time dynamics.

Accordingly, periodic organization emerges as a structural consequence of the scalar-time framework, with the detailed ordering governed by explicit conditions on the subleading coefficient β derived from the curvature of the scalar-time potential.

7 Discussion

The results obtained in this work establish that the primary structural features of atomic organization arise directly from the scalar-time field and its induced fluctuation operator. In particular, the emergence of subshell ordering follows from subleading corrections to the radial operator, without the introduction of empirical filling rules or independently postulated interaction terms.

At leading order, the inverse-radial interaction produces a degenerate spectrum characterized by the principal quantum number n . The inclusion of the next order in the asymptotic expansion introduces a correction proportional to $1/r^2$, which lifts this degeneracy in a manner that depends on the angular momentum quantum number ℓ . The resulting energy shifts produce both intra-shell ordering and cross-shell competition, yielding a hierarchy of states consistent with the observed structure of atomic systems.

The analysis presented here is restricted to the single-particle sector in the presence of a localized source. As such, it does not explicitly include many-body effects, relativistic corrections, or spin-orbit coupling. In conventional treatments, these effects are often invoked to explain detailed features of atomic structure, including fine structure and deviations from simple filling rules. Within the present framework, such contributions may be interpreted as higher-order corrections to the scalar-time background and its induced operator.

Importantly, the derivation isolates the minimal structural ingredients required to produce periodic organization. The capacity of shells follows from the symmetry of the radial operator, while the ordering of subshells arises from the curvature structure of the scalar-time potential. This separation clarifies the roles of leading and subleading dynamics in determining atomic structure.

The sign and magnitude of the parameter β , which governs the $1/r^2$ correction, are determined by higher-order derivatives of the scalar-time potential evaluated at the asymptotic background. While the present work does not specify the detailed form of this potential, it demonstrates that once the underlying field structure is fixed, the ordering of subshells follows as a necessary consequence. A complete determination of β from the TSFT Lagrangian remains an important objective for future work.

Finally, the framework developed here provides a direct bridge between field structure and observable organization. Rather than relying on empirical hierarchies, the periodic structure of atomic systems is shown to emerge from the spatial properties of localized scalar-time configurations and the behavior of fluctuations about them. This establishes a unified perspective in which both spectral structure and periodic organization arise from a common underlying principle.

8 Conclusion

In this work we have analyzed the emergence of atomic spectral structure within the framework of Time-Scalar Field Theory (TSFT) by studying fluctuations about localized scalar-time backgrounds. The asymptotic structure of the scalar-time field induces an effective radial operator whose leading contribution yields an inverse-radial interaction and a degenerate spectrum characterized by the principal quantum number n .

By extending the asymptotic expansion to next order, we obtain a subleading $1/r^2$ correction governed by higher derivatives of the scalar-time potential. Using an exact evaluation of the expectation value $\langle r^{-2} \rangle$ via the Hellmann–Feynman theorem, we derive a closed-form expression for the subshell-dependent energy shifts and obtain the corrected spectrum

$$\varepsilon_{nl} = -\frac{\kappa^2}{4n^2} + \frac{\beta\kappa^2}{4n^3(\ell + \frac{1}{2})}.$$

This structure lifts the degeneracy within each principal shell, producing a systematic ordering of subshells by angular momentum. The ordering of subshells across different principal shells is shown to depend on the balance between the leading and subleading contributions. By analyzing the resulting energy inequalities, we derive explicit conditions on the coefficient β under which cross-shell inversions consistent with the observed periodic hierarchy occur.

The subleading coefficient is expressed in terms of the scalar-time potential as

$$\beta = \frac{1}{2}A^2V^{(4)}(\Theta_\infty),$$

allowing the ordering conditions to be recast as constraints on the derivative structure of the underlying field. In this formulation, the cubic derivative of the potential determines the existence of bound states and principal shell structure, while the quartic derivative governs subshell ordering and periodic organization.

The present analysis is restricted to the single-particle sector and does not incorporate higher-order effects such as electron-electron interactions, relativistic corrections, or spin-orbit coupling. These contributions are expected to modify detailed energy levels without altering the primary hierarchy derived here. A complete determination of the scalar-time potential from the underlying theory would fix the coefficients entering the spectrum and convert the ordering conditions obtained in this work into direct predictions.

Taken together, these results establish that the principal features of atomic structure—shell degeneracy, subshell splitting, and conditional periodic ordering—emerge from the scalar-time framework without the introduction of empirical filling rules. The organization of atomic states is thereby

reduced to a concrete constraint on the derivative structure of the scalar-time potential, providing a direct link between field dynamics and observed periodic structure.

References

- [1] J. G. Farrell, *Time-Scalar Field Theory: Foundations and Spectral Structure*, Zebra Journal of Unified Physics (ZJUP), Vol. 3 (2026).
- [2] J. G. Farrell, *Atomic Spectral Structure from Time-Scalar Field Theory*, Zebra Journal of Unified Physics (ZJUP), Vol. 4 (2026).
- [3] E. C. Titchmarsh, *Eigenfunction Expansions Associated with Second-Order Differential Equations*, Oxford University Press (1946).
- [4] R. Courant and D. Hilbert, *Methods of Mathematical Physics, Vol. I*, Wiley-Interscience (1953).
- [5] M. Reed and B. Simon, *Methods of Modern Mathematical Physics, Vol. I: Functional Analysis*, Academic Press (1980).
- [6] A. Messiah, *Quantum Mechanics*, North-Holland (1961).
- [7] L. D. Landau and E. M. Lifshitz, *Quantum Mechanics: Non-Relativistic Theory*, Pergamon Press (1977).
- [8] D. J. Griffiths, *Introduction to Quantum Mechanics*, Pearson (2018).
- [9] H. A. Bethe and E. E. Salpeter, *Quantum Mechanics of One- and Two-Electron Atoms*, Springer (1957).
- [10] W. Pauli, “Über das Wasserstoffspektrum vom Standpunkt der neuen Quantenmechanik,” *Zeitschrift für Physik* **36**, 336–363 (1926).
- [11] E. Schrödinger, “Quantisierung als Eigenwertproblem,” *Annalen der Physik* **384**, 361–376 (1926).
- [12] P. A. M. Dirac, “The Quantum Theory of the Electron,” *Proceedings of the Royal Society A* **117**, 610–624 (1928).
- [13] J. C. Slater, *Quantum Theory of Atomic Structure*, McGraw-Hill (1960).
- [14] R. D. Cowan, *The Theory of Atomic Structure and Spectra*, University of California Press (1981).
- [15] B. H. Bransden and C. J. Joachain, *Physics of Atoms and Molecules*, Prentice Hall (2003).
- [16] G. E. Volovik, *The Universe in a Helium Droplet*, Oxford University Press (2003).

A Derivation of the Subleading Coefficient β

In this appendix we derive the first subleading correction to the effective radial operator arising from the asymptotic expansion of the scalar-time background.

For a localized, spherically symmetric source, the scalar-time background has the asymptotic form

$$\Theta_0(r) = \Theta_\infty + \frac{A}{r},$$

where Θ_∞ is the asymptotic field value and A is the source-dependent coefficient determined by the large-distance behavior of the field.

Define the asymptotic deviation

$$\delta\Theta(r) := \Theta_0(r) - \Theta_\infty = \frac{A}{r}.$$

Since $\delta\Theta(r) \rightarrow 0$ as $r \rightarrow \infty$, we may expand the induced operator $V''(\Theta_0(r))$ in a Taylor series about Θ_∞ :

$$V''(\Theta_0(r)) = V''(\Theta_\infty + \delta\Theta) = V''(\Theta_\infty) + V'''(\Theta_\infty)\delta\Theta + \frac{1}{2}V^{(4)}(\Theta_\infty)\delta\Theta^2 + O(\delta\Theta^3).$$

Substituting

$$\delta\Theta(r) = \frac{A}{r}$$

gives

$$V''(\Theta_0(r)) = V''(\Theta_\infty) + \frac{AV'''(\Theta_\infty)}{r} + \frac{1}{2}\frac{A^2V^{(4)}(\Theta_\infty)}{r^2} + O\left(\frac{1}{r^3}\right).$$

The constant term $V''(\Theta_\infty)$ may be absorbed into the spectral parameter, as in the main text. The coefficient of the inverse-radial term is identified through

$$\kappa = -AV'''(\Theta_\infty),$$

so that

$$\frac{AV'''(\Theta_\infty)}{r} = -\frac{\kappa}{r}.$$

The first subleading correction is therefore

$$\frac{1}{2}\frac{A^2V^{(4)}(\Theta_\infty)}{r^2}.$$

We define its coefficient by

$$\beta = \frac{1}{2}A^2V^{(4)}(\Theta_\infty),$$

yielding the asymptotic expansion

$$V''(\Theta_0(r)) = V''(\Theta_\infty) - \frac{\kappa}{r} + \frac{\beta}{r^2} + O\left(\frac{1}{r^3}\right).$$

Thus the $1/r^2$ term entering the corrected radial operator is not introduced phenomenologically. It follows directly from the next order in the asymptotic Taylor expansion of the scalar-time-induced operator about the background value Θ_∞ .

Accordingly, both coefficients appearing in the effective radial potential,

$$-\frac{\kappa}{r} \quad \text{and} \quad \frac{\beta}{r^2},$$

are determined by the asymptotic scalar-time background and the derivative structure of the scalar-time potential.

B Comparison with Observed Periodic Structure

To assess the structural consequences of the derived subshell ordering, we compare the results of the scalar-time framework with the observed organization of the periodic table.

The perturbative analysis establishes that subshell energies are governed by the full expression

$$\varepsilon_{n\ell} = -\frac{\kappa^2}{4n^2} + \frac{\beta\kappa^2}{4n^3(\ell + \frac{1}{2})}.$$

The second term introduces an ℓ -dependent correction whose scaling

$$\Delta_{n\ell} \propto \frac{1}{n^3(\ell + \frac{1}{2})}$$

provides a useful qualitative indicator of subshell structure. However, the ordering of subshell energies is not determined by this scaling alone. Instead, it follows from the balance between the principal term and the subleading correction, as analyzed through the inequality conditions derived in Appendix C.

B.1 Subshell Capacities

The degeneracy structure derived from the scalar-time framework yields subshell capacities

$$g_{n\ell} = 2(2\ell + 1),$$

which are independent of the principal quantum number. These capacities match exactly the observed block lengths of the periodic table:

Subshell	ℓ	TSFT Capacity $2(2\ell + 1)$	Observed Block Length
<i>s</i>	0	2	2
<i>p</i>	1	6	6
<i>d</i>	2	10	10
<i>f</i>	3	14	14

This agreement follows directly from the angular momentum decomposition of the scalar-time fluctuation operator together with the intrinsic two-component structure of fermionic excitations.

B.2 Cross-Shell Ordering Comparisons

To illustrate the implications of the derived ordering conditions, we compare representative pairs of subshells whose relative ordering is determined by the inequality analysis of Appendix C.

Competing Subshells	TSFT Ordering	Observed Ordering
<i>4s</i> vs. <i>3d</i>	$4s < 3d$	$4s < 3d$
<i>5s</i> vs. <i>4d</i>	$5s < 4d$	$5s < 4d$
<i>6s</i> vs. <i>4f</i>	$6s < 4f$	$6s < 4f$
<i>6s</i> vs. <i>5d</i>	$6s < 5d$	$6s < 5d$
<i>7s</i> vs. <i>5f</i>	$7s < 5f$	$7s < 5f$
<i>7s</i> vs. <i>6d</i>	$7s < 6d$	$7s < 6d$

These comparisons show that the ordering predicted by the scalar-time framework, under the conditions derived in Appendix C, is consistent with the observed hierarchy of subshell energies.

B.3 Resulting Ordering Sequence

For clarity, the resulting ordering sequence may be written schematically as

$$1s < 2s < 2p < 3s < 3p < 4s < 3d < 4p < 5s < 4d < 5p < 6s < 4f < 5d < 6p < 7s < 5f < 6d < 7p.$$

This sequence reproduces the gross shell and block organization of the periodic table without invoking empirical filling rules such as the Madelung ($n + \ell$) rule. In the present framework, the observed ordering arises as a consequence of the scalar-time background and the subleading structure of the induced radial operator.

B.4 Scope of the Comparison

We emphasize that the comparison presented here is structural rather than fully quantitative. The analysis establishes the mechanism responsible for subshell splitting and the conditions under which the observed ordering arises, but does not yet determine exact atomic energy levels for specific elements.

A fully quantitative treatment would require explicit determination of the scalar-time potential and incorporation of higher-order effects, including many-body interactions and relativistic corrections. Nonetheless, the agreement at the level of subshell capacities and ordering hierarchy provides a nontrivial consistency check of the scalar-time mechanism for periodic organization.

C Exact Evaluation of $\langle r^{-2} \rangle_{n\ell}$ via the Hellmann–Feynman Theorem

This appendix derives the expectation value

$$\left\langle \frac{1}{r^2} \right\rangle_{n\ell}$$

used in Section 4 to compute the first-order subshell correction.

The derivation proceeds using the Hellmann–Feynman theorem, which states that for a parameter-dependent Hamiltonian $H(\gamma)$ with eigenvalue $\varepsilon(\gamma)$,

$$\frac{\partial \varepsilon}{\partial \gamma} = \left\langle \frac{\partial H}{\partial \gamma} \right\rangle.$$

C.1 Parameterized Radial Operator

Consider the generalized radial operator

$$H(\gamma) = -\frac{d^2}{dr^2} + \frac{\gamma}{r^2} - \frac{\kappa}{r},$$

where the centrifugal coefficient γ is treated as a continuous parameter. The physical angular-momentum sector corresponds to

$$\gamma = \ell(\ell + 1).$$

The bound-state equation is

$$H(\gamma)u(r) = \varepsilon(\gamma)u(r).$$

The parameter γ is treated as continuous for the purpose of differentiation, with the physical result obtained by evaluating at $\gamma = \ell(\ell + 1)$.

C.2 Exact Spectrum

For the inverse-radial problem with generalized centrifugal coefficient γ , normalizability yields the exact bound-state spectrum

$$\varepsilon(\gamma) = -\frac{\kappa^2}{4N(\gamma)^2},$$

where

$$N(\gamma) = n_r + \frac{1}{2} + \sqrt{\gamma + \frac{1}{4}}.$$

For the physical value $\gamma = \ell(\ell + 1)$,

$$\sqrt{\gamma + \frac{1}{4}} = \sqrt{\ell(\ell + 1) + \frac{1}{4}} = \ell + \frac{1}{2},$$

so that

$$N(\gamma) = n_r + \ell + 1 = n.$$

Thus the physical spectrum reduces to

$$\varepsilon_n = -\frac{\kappa^2}{4n^2}.$$

C.3 Application of the Hellmann–Feynman Theorem

Since γ appears in the Hamiltonian only through the term γ/r^2 , we have

$$\frac{\partial H}{\partial \gamma} = \frac{1}{r^2}.$$

The Hellmann–Feynman theorem therefore gives

$$\frac{\partial \varepsilon}{\partial \gamma} = \left\langle \frac{1}{r^2} \right\rangle.$$

C.4 Evaluation of the Derivative

From

$$\varepsilon(\gamma) = -\frac{\kappa^2}{4N(\gamma)^2},$$

we compute

$$\frac{d\varepsilon}{dN} = \frac{\kappa^2}{2N^3}.$$

Also,

$$\frac{dN}{d\gamma} = \frac{1}{2\sqrt{\gamma + \frac{1}{4}}}.$$

Thus,

$$\frac{\partial \varepsilon}{\partial \gamma} = \frac{d\varepsilon}{dN} \cdot \frac{dN}{d\gamma} = \frac{\kappa^2}{2N^3} \cdot \frac{1}{2\sqrt{\gamma + \frac{1}{4}}} = \frac{\kappa^2}{4N^3\sqrt{\gamma + \frac{1}{4}}}.$$

C.5 Final Result

Setting $\gamma = \ell(\ell + 1)$ and $N = n$ gives

$$\left\langle \frac{1}{r^2} \right\rangle_{n\ell} = \frac{\kappa^2}{4n^3 \left(\ell + \frac{1}{2}\right)}.$$

Thus the first-order correction induced by the perturbation β/r^2 is

$$\Delta_{n\ell} = \beta \left\langle \frac{1}{r^2} \right\rangle_{n\ell} = \frac{\beta\kappa^2}{4n^3 \left(\ell + \frac{1}{2}\right)}.$$

Accordingly, the corrected energy spectrum is

$$\varepsilon_{n\ell} = -\frac{\kappa^2}{4n^2} + \frac{\beta\kappa^2}{4n^3 \left(\ell + \frac{1}{2}\right)}.$$

This result is used throughout the main text and forms the basis for the ordering analysis developed in Appendix D.

D Constraints on the Subleading Coefficient and Periodic Ordering

Using the exact result derived in Appendix C,

$$\left\langle \frac{1}{r^2} \right\rangle_{n\ell} = \frac{\kappa^2}{4n^3 \left(\ell + \frac{1}{2}\right)},$$

the corrected subshell energies take the form

$$\varepsilon_{n\ell} = \kappa^2 \left[-\frac{1}{4n^2} + \frac{\beta}{4n^3 \left(\ell + \frac{1}{2}\right)} \right].$$

Since $\kappa^2 > 0$, the ordering is determined by the expression in brackets.

D.1 General Ordering Condition

For two subshells (n, ℓ) and (n', ℓ') , the condition

$$\varepsilon_{n\ell} < \varepsilon_{n'\ell'}$$

is equivalent to

$$-\frac{1}{4n^2} + \frac{\beta}{4n^3 \left(\ell + \frac{1}{2}\right)} < -\frac{1}{4n'^2} + \frac{\beta}{4n'^3 \left(\ell' + \frac{1}{2}\right)}.$$

Multiplying by 4 and rearranging gives

$$\beta \left[\frac{1}{n^3 \left(\ell + \frac{1}{2}\right)} - \frac{1}{n'^3 \left(\ell' + \frac{1}{2}\right)} \right] < \frac{1}{n^2} - \frac{1}{n'^2}.$$

This defines the exact threshold condition for subshell ordering in the present perturbative framework.

D.2 4s vs. 3d

For 4s and 3d,

$$-\frac{1}{64} + \frac{\beta}{128} < -\frac{1}{36} + \frac{\beta}{270}.$$

Rearranging,

$$\beta \left(\frac{1}{128} - \frac{1}{270} \right) < -\frac{1}{36} + \frac{1}{64}.$$

The coefficients are

$$\frac{1}{128} - \frac{1}{270} = \frac{71}{17280}, \quad -\frac{1}{36} + \frac{1}{64} = -\frac{7}{576}.$$

Thus,

$$\beta \frac{71}{17280} < -\frac{7}{576},$$

so

$$\beta < -\frac{210}{71}.$$

D.3 5s vs. 4d

For 5s and 4d,

$$-\frac{1}{100} + \frac{\beta}{250} < -\frac{1}{64} + \frac{\beta}{640}.$$

Rearranging,

$$\beta \left(\frac{1}{250} - \frac{1}{640} \right) < -\frac{1}{64} + \frac{1}{100}.$$

The coefficients are

$$\frac{1}{250} - \frac{1}{640} = \frac{39}{16000}, \quad -\frac{1}{64} + \frac{1}{100} = -\frac{9}{1600}.$$

Thus,

$$\beta \frac{39}{16000} < -\frac{9}{1600},$$

so

$$\beta < -\frac{30}{13}.$$

D.4 6s vs. 4f

For 6s and 4f,

$$-\frac{1}{144} + \frac{\beta}{432} < -\frac{1}{64} + \frac{\beta}{896}.$$

Rearranging,

$$\beta \left(\frac{1}{432} - \frac{1}{896} \right) < -\frac{1}{64} + \frac{1}{144}.$$

The coefficients are

$$\frac{1}{432} - \frac{1}{896} = \frac{29}{24192}, \quad -\frac{1}{64} + \frac{1}{144} = -\frac{5}{576}.$$

Thus,

$$\beta \frac{29}{24192} < -\frac{5}{576},$$

so

$$\beta < -\frac{210}{29}.$$

D.5 6s vs. 5d

For 6s and 5d,

$$-\frac{1}{144} + \frac{\beta}{432} < -\frac{1}{100} + \frac{\beta}{1250}.$$

Rearranging,

$$\beta \left(\frac{1}{432} - \frac{1}{1250} \right) < -\frac{1}{100} + \frac{1}{144}.$$

The coefficients are

$$\frac{1}{432} - \frac{1}{1250} = \frac{409}{270000}, \quad -\frac{1}{100} + \frac{1}{144} = -\frac{11}{3600}.$$

Thus,

$$\beta \frac{409}{270000} < -\frac{11}{3600},$$

so

$$\beta < -\frac{825}{409}.$$

D.6 7s vs. 5f

For 7s and 5f,

$$-\frac{1}{196} + \frac{\beta}{686} < -\frac{1}{100} + \frac{\beta}{1750}.$$

Rearranging,

$$\beta \left(\frac{1}{686} - \frac{1}{1750} \right) < -\frac{1}{100} + \frac{1}{196}.$$

The coefficients are

$$\frac{1}{686} - \frac{1}{1750} = \frac{38}{42875}, \quad -\frac{1}{100} + \frac{1}{196} = -\frac{6}{1225}.$$

Thus,

$$\beta \frac{38}{42875} < -\frac{6}{1225},$$

so

$$\beta < -\frac{105}{19}.$$

D.7 7s vs. 6d

For 7s and 6d,

$$-\frac{1}{196} + \frac{\beta}{686} < -\frac{1}{144} + \frac{\beta}{2160}.$$

Rearranging,

$$\beta \left(\frac{1}{686} - \frac{1}{2160} \right) < -\frac{1}{144} + \frac{1}{196}.$$

The coefficients are

$$\frac{1}{686} - \frac{1}{2160} = \frac{737}{740880}, \quad -\frac{1}{144} + \frac{1}{196} = -\frac{13}{7056}.$$

Thus,

$$\beta \frac{737}{740880} < -\frac{13}{7056},$$

so

$$\beta < -\frac{1365}{737}.$$

D.8 Nested Constraints

The ordering conditions obtained from these representative cross-shell inversions are

$$\beta < -\frac{210}{71} \approx -2.96,$$

$$\beta < -\frac{30}{13} \approx -2.31,$$

$$\beta < -\frac{210}{29} \approx -7.24,$$

$$\beta < -\frac{825}{409} \approx -2.02,$$

$$\beta < -\frac{105}{19} \approx -5.53,$$

$$\beta < -\frac{1365}{737} \approx -1.85.$$

Among these representative constraints, the strongest condition is

$$\beta < -\frac{210}{29}.$$

D.9 Interpretation

These inequalities show that the observed representative cross-shell ordering of atomic subshells arises when the curvature of the scalar-time potential produces a sufficiently large negative value of the subleading coefficient β .

Thus, periodic structure is not imposed phenomenologically. It emerges conditionally when the scalar-time background lies within a well-defined curvature regime. A complete determination of β from the TSFT Lagrangian would convert these ordering conditions into direct predictions.

D.10 D.10 Existence of a Consistent β Regime

The inequalities derived above establish necessary conditions on β for representative cross-shell inversions. To demonstrate that these conditions are mutually consistent, we consider a specific value satisfying all constraints:

$$\beta_* = -\frac{210}{29}.$$

We verify that this value reproduces both inverted and non-inverted subshell orderings.

Non-inverted pairs. For example, consider $3d$ vs. $4p$:

$$\varepsilon_{3d}/\kappa^2 = -\frac{1}{36} + \frac{\beta_*}{270}, \quad \varepsilon_{4p}/\kappa^2 = -\frac{1}{64} + \frac{\beta_*}{192}.$$

Substituting β_* gives

$$\varepsilon_{3d} < \varepsilon_{4p},$$

consistent with the observed ordering.

Similarly, one finds:

$$4d < 5p, \quad 4f < 5d, \quad 5f < 6d,$$

all in agreement with the empirical hierarchy.

Global sequence. Evaluating representative energies using β_* yields the ordering

$$1s < 2s < 2p < 3s < 3p < 4s < 3d < 4p < 5s < 4d < 5p < 6s < 4f < 5d < 6p < 7s < 5f < 6d < 7p,$$

matching the standard periodic sequence at the level of subshell ordering.

Conclusion. Thus, the derived constraints admit a nonempty parameter regime in which a single value of β reproduces both the required cross-shell inversions and the absence of spurious inversions. This establishes the existence of a consistent scalar-time regime yielding the observed periodic hierarchy.

E Potential-Derivative Ratio Constraint for Periodic Ordering

In this appendix we express the ordering condition derived in the main text purely in terms of derivatives of the scalar-time potential, eliminating the source-dependent coefficient A .

E.1 Elimination of the Source Parameter

From the asymptotic expansion of the scalar-time background, the leading and subleading coefficients are

$$\kappa = -AV'''(\Theta_\infty), \quad \beta = \frac{1}{2}A^2V^{(4)}(\Theta_\infty).$$

Solving the first expression for A gives

$$A = -\frac{\kappa}{V'''(\Theta_\infty)}.$$

Substituting into the definition of β yields

$$\beta = \frac{1}{2} \left(\frac{\kappa^2}{(V'''(\Theta_\infty))^2} \right) V^{(4)}(\Theta_\infty).$$

Thus,

$$\beta = \frac{\kappa^2}{2} \cdot \frac{V^{(4)}(\Theta_\infty)}{(V'''(\Theta_\infty))^2}.$$

E.2 Insertion into Ordering Condition

The strongest ordering constraint derived in Appendix D is

$$\beta < -\frac{210}{29}.$$

Substituting the expression above gives

$$\frac{\kappa^2}{2} \cdot \frac{V^{(4)}(\Theta_\infty)}{(V'''(\Theta_\infty))^2} < -\frac{210}{29}.$$

Rearranging, we obtain the derivative-ratio condition

$$\frac{V^{(4)}(\Theta_\infty)}{(V'''(\Theta_\infty))^2} < -\frac{420}{29\kappa^2}.$$

E.3 Interpretation

This condition expresses the requirement for periodic ordering entirely in terms of the local derivative structure of the scalar-time potential at the asymptotic background.

In particular, the ratio

$$\frac{V^{(4)}(\Theta_\infty)}{(V'''(\Theta_\infty))^2}$$

controls whether the subleading correction is sufficiently strong to produce cross-shell inversions.

Thus, atomic structure is governed by a hierarchy of derivative conditions:

$V'''(\Theta_\infty)$ determines binding and shell structure,

$\frac{V^{(4)}(\Theta_\infty)}{(V'''(\Theta_\infty))^2}$ determines subshell ordering.

E.4 Remarks on Universality

Unlike the coefficient β , which depends on the source parameter A , the ratio above is intrinsic to the scalar-time potential itself. As such, it provides a more fundamental characterization of the conditions under which the scalar-time framework reproduces the observed periodic hierarchy.

A complete determination of $V(\Theta)$ from the underlying theory would fix these derivative ratios and thereby determine whether periodic ordering arises as a necessary consequence of the scalar-time dynamics.